Measurement of Branching Fractions and *CP* and Isospin Asymmetries in $B \rightarrow K^*(892)\gamma$ Decays

(The *BaBar* Collaboration)

B. Aubert,[1] Y. Karyotakis,[1] J. P. Lees,[1] V. Poireau,[1] E. Prencipe,[1] X. Prudent,[1] V. Tisserand,[1] J. Garra Tico,[2] E. Grauges,[2] M. Martinelli[ab],[3] A. Palano[ab],[3] M. Pappagallo[ab],[3] G. Eigen,[4] B. Stugu,[4] L. Sun,[4] M. Battaglia,[5] D. N. Brown,[5] L. T. Kerth,[5] Yu. G. Kolomensky,[5] G. Lynch,[5] I. L. Osipenkov,[5] K. Tackmann,[5] T. Tanabe,[5] C. M. Hawkes,[6] N. Soni,[6] A. T. Watson,[6] H. Koch,[7] T. Schroeder,[7] D. J. Asgeirsson,[8] B. G. Fulsom,[8] C. Hearty,[8] T. S. Mattison,[8] J. A. McKenna,[8] M. Barrett,[9] A. Khan,[9] A. Randle-Conde,[9] V. E. Blinov,[10] A. D. Bukin,[10, *] A. R. Buzykaev,[10] V. P. Druzhinin,[10] V. B. Golubev,[10] A. P. Onuchin,[10] S. I. Serednyakov,[10] Yu. I. Skovpen,[10] E. P. Solodov,[10] K. Yu. Todyshev,[10] M. Bondioli,[11] S. Curry,[11] I. Eschrich,[11] D. Kirkby,[11] A. J. Lankford,[11] P. Lund,[11] M. Mandelkern,[11] E. C. Martin,[11] D. P. Stoker,[11] H. Atmacan,[12] J. W. Gary,[12] F. Liu,[12] O. Long,[12] G. M. Vitug,[12] Z. Yasin,[12] L. Zhang,[12] V. Sharma,[13] C. Campagnari,[14] T. M. Hong,[14] D. Kovalskyi,[14] M. A. Mazur,[14] J. D. Richman,[14] T. W. Beck,[15] A. M. Eisner,[15] C. A. Heusch,[15] J. Kroseberg,[15] W. S. Lockman,[15] A. J. Martinez,[15] T. Schalk,[15] B. A. Schumm,[15] A. Seiden,[15] L. Wang,[15] L. O. Winstrom,[15] C. H. Cheng,[16] D. A. Doll,[16] B. Echenard,[16] F. Fang,[16] D. G. Hitlin,[16] I. Narsky,[16] T. Piatenko,[16] F. C. Porter,[16] R. Andreassen,[17] G. Mancinelli,[17] B. T. Meadows,[17] K. Mishra,[17] M. D. Sokoloff,[17] P. C. Bloom,[18] W. T. Ford,[18] A. Gaz,[18] J. F. Hirschauer,[18] M. Nagel,[18] U. Nauenberg,[18] J. G. Smith,[18] S. R. Wagner,[18] R. Ayad,[19, †] W. H. Toki,[19] R. J. Wilson,[19] E. Feltresi,[20] A. Hauke,[20] H. Jasper,[20] T. M. Karbach,[20] J. Merkel,[20] A. Petzold,[20] B. Spaan,[20] K. Wacker,[20] M. J. Kobel,[21] R. Nogowski,[21] K. R. Schubert,[21] R. Schwierz,[21] A. Volk,[21] D. Bernard,[22] E. Latour,[22] M. Verderi,[22] P. J. Clark,[23] S. Playfer,[23] J. E. Watson,[23] M. Andreotti[ab],[24] D. Bettoni[a],[24] C. Bozzi[a],[24] R. Calabrese[ab],[24] A. Cecchi[ab],[24] G. Cibinetto[ab],[24] E. Fioravanti[ab],[24] P. Franchini[ab],[24] E. Luppi[ab],[24] M. Munerato[ab],[24] M. Negrini[ab],[24] A. Petrella[ab],[24] L. Piemontese[a],[24] V. Santoro[ab],[24] R. Baldini-Ferroli,[25] A. Calcaterra,[25] R. de Sangro,[25] G. Finocchiaro,[25] S. Pacetti,[25] P. Patteri,[25] I. M. Peruzzi,[25, ‡] M. Piccolo,[25] M. Rama,[25] A. Zallo,[25] R. Contri[ab],[26] E. Guido,[26] M. Lo Vetere[ab],[26] M. R. Monge[ab],[26] S. Passaggio[a],[26] C. Patrignani[ab],[26] E. Robutti[a],[26] S. Tosi[ab],[26] K. S. Chaisanguanthum,[27] M. Morii,[27] A. Adametz,[28] J. Marks,[28] S. Schenk,[28] U. Uwer,[28] F. U. Bernlochner,[29] V. Klose,[29] H. M. Lacker,[29] D. J. Bard,[30] P. D. Dauncey,[30] M. Tibbetts,[30] P. K. Behera,[31] M. J. Charles,[31] U. Mallik,[31] J. Cochran,[32] H. B. Crawley,[32] L. Dong,[32] V. Eyges,[32] W. T. Meyer,[32] S. Prell,[32] E. I. Rosenberg,[32] A. E. Rubin,[32] Y. Y. Gao,[33] A. V. Gritsan,[33] Z. J. Guo,[33] N. Arnaud,[34] J. Béquilleux,[34] A. D'Orazio,[34] M. Davier,[34] D. Derkach,[34] J. Firmino da Costa,[34] G. Grosdidier,[34] F. Le Diberder,[34] V. Lepeltier,[34] A. M. Lutz,[34] B. Malaescu,[34] S. Pruvot,[34] P. Roudeau,[34] M. H. Schune,[34] J. Serrano,[34] V. Sordini,[34, §] A. Stocchi,[34] G. Wormser,[34] D. J. Lange,[35] D. M. Wright,[35] I. Bingham,[36] J. P. Burke,[36] C. A. Chavez,[36] J. R. Fry,[36] E. Gabathuler,[36] R. Gamet,[36] D. E. Hutchcroft,[36] D. J. Payne,[36] C. Touramanis,[36] A. J. Bevan,[37] C. K. Clarke,[37] F. Di Lodovico,[37] R. Sacco,[37] M. Sigamani,[37] G. Cowan,[38] S. Paramesvaran,[38] A. C. Wren,[38] D. N. Brown,[39] C. L. Davis,[39] A. G. Denig,[40] M. Fritsch,[40] W. Gradl,[40] A. Hafner,[40] K. E. Alwyn,[41] D. Bailey,[41] R. J. Barlow,[41] G. Jackson,[41] G. D. Lafferty,[41] T. J. West,[41] J. I. Yi,[41] J. Anderson,[42] C. Chen,[42] A. Jawahery,[42] D. A. Roberts,[42] G. Simi,[42] J. M. Tuggle,[42] C. Dallapiccola,[43] E. Salvati,[43] S. Saremi,[43] R. Cowan,[44] D. Dujmic,[44] P. H. Fisher,[44] S. W. Henderson,[44] G. Sciolla,[44] M. Spitznagel,[44] R. K. Yamamoto,[44] M. Zhao,[44] P. M. Patel,[45] S. H. Robertson,[45] M. Schram,[45] A. Lazzaro[ab],[46] V. Lombardo[a],[46] F. Palombo[ab],[46] S. Stracka[ab],[46] J. M. Bauer,[47] L. Cremaldi,[47] R. Godang,[47, ¶] R. Kroeger,[47] P. Sonnek,[47] D. J. Summers,[47] H. W. Zhao,[47] M. Simard,[48] P. Taras,[48] H. Nicholson,[49] G. De Nardo[ab],[50] L. Lista[a],[50] D. Monorchio[ab],[50] G. Onorato[ab],[50] C. Sciacca[ab],[50] G. Raven,[51] H. L. Snoek,[51] C. P. Jessop,[52] K. J. Knoepfel,[52] J. M. LoSecco,[52] W. F. Wang,[52] L. A. Corwin,[53] K. Honscheid,[53] H. Kagan,[53] R. Kass,[53] J. P. Morris,[53] A. M. Rahimi,[53] J. J. Regensburger,[53] S. J. Sekula,[53] Q. K. Wong,[53] N. L. Blount,[54] J. Brau,[54] R. Frey,[54] O. Igonkina,[54] J. A. Kolb,[54] M. Lu,[54] R. Rahmat,[54] N. B. Sinev,[54] D. Strom,[54] J. Strube,[54] E. Torrence,[54] G. Castelli[ab],[55] N. Gagliardi[ab],[55] M. Margoni[ab],[55] M. Morandin[a],[55] M. Posocco[a],[55] M. Rotondo[a],[55] F. Simonetto[ab],[55] R. Stroili[ab],[55] C. Voci[ab],[55] P. del Amo Sanchez,[56] E. Ben-Haim,[56] G. R. Bonneaud,[56] H. Briand,[56] J. Chauveau,[56] O. Hamon,[56] Ph. Leruste,[56] G. Marchiori,[56] J. Ocariz,[56]

A. Perez,[56] J. Prendki,[56] S. Sitt,[56] L. Gladney,[57] M. Biasini[ab,58] E. Manoni[ab,58] C. Angelini[ab,59] G. Batignani[ab,59] S. Bettarini[ab,59] G. Calderini[ab,59,**] M. Carpinelli[ab,59,††] A. Cervelli[ab,59] F. Forti[ab,59] M. A. Giorgi[ab,59] A. Lusiani[ac,59] M. Morganti[ab,59] N. Neri[ab,59] E. Paoloni[ab,59] G. Rizzo[ab,59] J. J. Walsh[a,59] D. Lopes Pegna,[60] C. Lu,[60] J. Olsen,[60] A. J. S. Smith,[60] A. V. Telnov,[60] F. Anulli[a,61] E. Baracchini[ab,61] G. Cavoto[a,61] R. Faccini[ab,61] F. Ferrarotto[a,61] F. Ferroni[ab,61] M. Gaspero[ab,61] P. D. Jackson[a,61] L. Li Gioi[a,61] M. A. Mazzoni[a,61] S. Morganti[a,61] G. Piredda[a,61] F. Renga[ab,61] C. Voena[a,61] M. Ebert,[62] T. Hartmann,[62] H. Schröder,[62] R. Waldi,[62] T. Adye,[63] B. Franek,[63] E. O. Olaiya,[63] F. F. Wilson,[63] S. Emery,[64] L. Esteve,[64] G. Hamel de Monchenault,[64] W. Kozanecki,[64] G. Vasseur,[64] Ch. Yèche,[64] M. Zito,[64] M. T. Allen,[65] D. Aston,[65] R. Bartoldus,[65] J. F. Benitez,[65] R. Cenci,[65] J. P. Coleman,[65] M. R. Convery,[65] J. C. Dingfelder,[65] J. Dorfan,[65] G. P. Dubois-Felsmann,[65] W. Dunwoodie,[65] R. C. Field,[65] M. Franco Sevilla,[65] A. M. Gabareen,[65] M. T. Graham,[65] P. Grenier,[65] C. Hast,[65] W. R. Innes,[65] J. Kaminski,[65] M. H. Kelsey,[65] H. Kim,[65] P. Kim,[65] M. L. Kocian,[65] D. W. G. S. Leith,[65] S. Li,[65] B. Lindquist,[65] S. Luitz,[65] V. Luth,[65] H. L. Lynch,[65] D. B. MacFarlane,[65] H. Marsiske,[65] R. Messner,[65,*] D. R. Muller,[65] H. Neal,[65] S. Nelson,[65] C. P. O'Grady,[65] I. Ofte,[65] M. Perl,[65] B. N. Ratcliff,[65] A. Roodman,[65] A. A. Salnikov,[65] R. H. Schindler,[65] J. Schwiening,[65] A. Snyder,[65] D. Su,[65] M. K. Sullivan,[65] K. Suzuki,[65] S. K. Swain,[65] J. M. Thompson,[65] J. Va'vra,[65] A. P. Wagner,[65] M. Weaver,[65] C. A. West,[65] W. J. Wisniewski,[65] M. Wittgen,[65] D. H. Wright,[65] H. W. Wulsin,[65] A. K. Yarritu,[65] C. C. Young,[65] V. Ziegler,[65] X. R. Chen,[66] H. Liu,[66] W. Park,[66] M. V. Purohit,[66] R. M. White,[66] J. R. Wilson,[66] P. R. Burchat,[67] A. J. Edwards,[67] T. S. Miyashita,[67] S. Ahmed,[68] M. S. Alam,[68] J. A. Ernst,[68] B. Pan,[68] M. A. Saeed,[68] S. B. Zain,[68] A. Soffer,[69] S. M. Spanier,[70] B. J. Wogsland,[70] R. Eckmann,[71] J. L. Ritchie,[71] A. M. Ruland,[71] C. J. Schilling,[71] R. F. Schwitters,[71] B. C. Wray,[71] B. W. Drummond,[72] J. M. Izen,[72] X. C. Lou,[72] F. Bianchi[ab,73] D. Gamba[ab,73] M. Pelliccioni[ab,73] M. Bomben[ab,74] L. Bosisio[ab,74] C. Cartaro[ab,74] G. Della Ricca[ab,74] L. Lanceri[ab,74] L. Vitale[ab,74] V. Azzolini,[75] N. Lopez-March,[75] F. Martinez-Vidal,[75] D. A. Milanes,[75] A. Oyanguren,[75] J. Albert,[76] Sw. Banerjee,[76] B. Bhuyan,[76] H. H. F. Choi,[76] K. Hamano,[76] G. J. King,[76] R. Kowalewski,[76] M. J. Lewczuk,[76] I. M. Nugent,[76] J. M. Roney,[76] R. J. Sobie,[76] T. J. Gershon,[77] P. F. Harrison,[77] J. Ilic,[77] T. E. Latham,[77] G. B. Mohanty,[77] E. M. T. Puccio,[77] H. R. Band,[78] X. Chen,[78] S. Dasu,[78] K. T. Flood,[78] Y. Pan,[78] R. Prepost,[78] C. O. Vuosalo,[78] and S. L. Wu[78]

[1]*Laboratoire d'Annecy-le-Vieux de Physique des Particules (LAPP), Université de Savoie, CNRS/IN2P3, F-74941 Annecy-Le-Vieux, France*
[2]*Universitat de Barcelona, Facultat de Fisica, Departament ECM, E-08028 Barcelona, Spain*
[3]*INFN Sezione di Bari[a]; Dipartimento di Fisica, Università di Bari[b], I-70126 Bari, Italy*
[4]*University of Bergen, Institute of Physics, N-5007 Bergen, Norway*
[5]*Lawrence Berkeley National Laboratory and University of California, Berkeley, California 94720, USA*
[6]*University of Birmingham, Birmingham, B15 2TT, United Kingdom*
[7]*Ruhr Universität Bochum, Institut für Experimentalphysik 1, D-44780 Bochum, Germany*
[8]*University of British Columbia, Vancouver, British Columbia, Canada V6T 1Z1*
[9]*Brunel University, Uxbridge, Middlesex UB8 3PH, United Kingdom*
[10]*Budker Institute of Nuclear Physics, Novosibirsk 630090, Russia*
[11]*University of California at Irvine, Irvine, California 92697, USA*
[12]*University of California at Riverside, Riverside, California 92521, USA*
[13]*University of California at San Diego, La Jolla, California 92093, USA*
[14]*University of California at Santa Barbara, Santa Barbara, California 93106, USA*
[15]*University of California at Santa Cruz, Institute for Particle Physics, Santa Cruz, California 95064, USA*
[16]*California Institute of Technology, Pasadena, California 91125, USA*
[17]*University of Cincinnati, Cincinnati, Ohio 45221, USA*
[18]*University of Colorado, Boulder, Colorado 80309, USA*
[19]*Colorado State University, Fort Collins, Colorado 80523, USA*
[20]*Technische Universität Dortmund, Fakultät Physik, D-44221 Dortmund, Germany*
[21]*Technische Universität Dresden, Institut für Kern- und Teilchenphysik, D-01062 Dresden, Germany*
[22]*Laboratoire Leprince-Ringuet, CNRS/IN2P3, Ecole Polytechnique, F-91128 Palaiseau, France*
[23]*University of Edinburgh, Edinburgh EH9 3JZ, United Kingdom*
[24]*INFN Sezione di Ferrara[a]; Dipartimento di Fisica, Università di Ferrara[b], I-44100 Ferrara, Italy*
[25]*INFN Laboratori Nazionali di Frascati, I-00044 Frascati, Italy*
[26]*INFN Sezione di Genova[a]; Dipartimento di Fisica, Università di Genova[b], I-16146 Genova, Italy*
[27]*Harvard University, Cambridge, Massachusetts 02138, USA*
[28]*Universität Heidelberg, Physikalisches Institut, Philosophenweg 12, D-69120 Heidelberg, Germany*
[29]*Humboldt-Universität zu Berlin, Institut für Physik, Newtonstr. 15, D-12489 Berlin, Germany*
[30]*Imperial College London, London, SW7 2AZ, United Kingdom*
[31]*University of Iowa, Iowa City, Iowa 52242, USA*
[32]*Iowa State University, Ames, Iowa 50011-3160, USA*

[33] *Johns Hopkins University, Baltimore, Maryland 21218, USA*
[34] *Laboratoire de l'Accélérateur Linéaire, IN2P3/CNRS et Université Paris-Sud 11,*
Centre Scientifique d'Orsay, B. P. 34, F-91898 Orsay Cedex, France
[35] *Lawrence Livermore National Laboratory, Livermore, California 94550, USA*
[36] *University of Liverpool, Liverpool L69 7ZE, United Kingdom*
[37] *Queen Mary, University of London, London, E1 4NS, United Kingdom*
[38] *University of London, Royal Holloway and Bedford New College, Egham, Surrey TW20 0EX, United Kingdom*
[39] *University of Louisville, Louisville, Kentucky 40292, USA*
[40] *Johannes Gutenberg-Universität Mainz, Institut für Kernphysik, D-55099 Mainz, Germany*
[41] *University of Manchester, Manchester M13 9PL, United Kingdom*
[42] *University of Maryland, College Park, Maryland 20742, USA*
[43] *University of Massachusetts, Amherst, Massachusetts 01003, USA*
[44] *Massachusetts Institute of Technology, Laboratory for Nuclear Science, Cambridge, Massachusetts 02139, USA*
[45] *McGill University, Montréal, Québec, Canada H3A 2T8*
[46] *INFN Sezione di Milano^a; Dipartimento di Fisica, Università di Milano^b, I-20133 Milano, Italy*
[47] *University of Mississippi, University, Mississippi 38677, USA*
[48] *Université de Montréal, Physique des Particules, Montréal, Québec, Canada H3C 3J7*
[49] *Mount Holyoke College, South Hadley, Massachusetts 01075, USA*
[50] *INFN Sezione di Napoli^a; Dipartimento di Scienze Fisiche,*
Università di Napoli Federico II^b, I-80126 Napoli, Italy
[51] *NIKHEF, National Institute for Nuclear Physics and High Energy Physics, NL-1009 DB Amsterdam, The Netherlands*
[52] *University of Notre Dame, Notre Dame, Indiana 46556, USA*
[53] *Ohio State University, Columbus, Ohio 43210, USA*
[54] *University of Oregon, Eugene, Oregon 97403, USA*
[55] *INFN Sezione di Padova^a; Dipartimento di Fisica, Università di Padova^b, I-35131 Padova, Italy*
[56] *Laboratoire de Physique Nucléaire et de Hautes Energies,*
IN2P3/CNRS, Université Pierre et Marie Curie-Paris6,
Université Denis Diderot-Paris7, F-75252 Paris, France
[57] *University of Pennsylvania, Philadelphia, Pennsylvania 19104, USA*
[58] *INFN Sezione di Perugia^a; Dipartimento di Fisica, Università di Perugia^b, I-06100 Perugia, Italy*
[59] *INFN Sezione di Pisa^a; Dipartimento di Fisica,*
Università di Pisa^b; Scuola Normale Superiore di Pisa^c, I-56127 Pisa, Italy
[60] *Princeton University, Princeton, New Jersey 08544, USA*
[61] *INFN Sezione di Roma^a; Dipartimento di Fisica,*
Università di Roma La Sapienza^b, I-00185 Roma, Italy
[62] *Universität Rostock, D-18051 Rostock, Germany*
[63] *Rutherford Appleton Laboratory, Chilton, Didcot, Oxon, OX11 0QX, United Kingdom*
[64] *CEA, Irfu, SPP, Centre de Saclay, F-91191 Gif-sur-Yvette, France*
[65] *SLAC National Accelerator Laboratory, Stanford, California 94309 USA*
[66] *University of South Carolina, Columbia, South Carolina 29208, USA*
[67] *Stanford University, Stanford, California 94305-4060, USA*
[68] *State University of New York, Albany, New York 12222, USA*
[69] *Tel Aviv University, School of Physics and Astronomy, Tel Aviv, 69978, Israel*
[70] *University of Tennessee, Knoxville, Tennessee 37996, USA*
[71] *University of Texas at Austin, Austin, Texas 78712, USA*
[72] *University of Texas at Dallas, Richardson, Texas 75083, USA*
[73] *INFN Sezione di Torino^a; Dipartimento di Fisica Sperimentale, Università di Torino^b, I-10125 Torino, Italy*
[74] *INFN Sezione di Trieste^a; Dipartimento di Fisica, Università di Trieste^b, I-34127 Trieste, Italy*
[75] *IFIC, Universitat de Valencia-CSIC, E-46071 Valencia, Spain*
[76] *University of Victoria, Victoria, British Columbia, Canada V8W 3P6*
[77] *Department of Physics, University of Warwick, Coventry CV4 7AL, United Kingdom*
[78] *University of Wisconsin, Madison, Wisconsin 53706, USA*
(Dated: October 31, 2018)

We present an analysis of the decays $B^0 \to K^{*0}(892)\gamma$ and $B^+ \to K^{*+}(892)\gamma$ using a sample of about 383 million $B\overline{B}$ events collected with the *BABAR* detector at the PEP-II asymmetric energy B factory. We measure the branching fractions $\mathcal{B}(B^0 \to K^{*0}\gamma) = (4.47 \pm 0.10 \pm 0.16) \times 10^{-5}$ and $\mathcal{B}(B^+ \to K^{*+}\gamma) = (4.22 \pm 0.14 \pm 0.16) \times 10^{-5}$. We constrain the direct CP asymmetry to be $-0.033 < \mathcal{A}(B \to K^*\gamma) < 0.028$ and the isospin asymmetry to be $0.017 < \Delta_{0-} < 0.116$, where the limits are determined by the 90% confidence interval and include both the statistical and systematic uncertainties.

PACS numbers:

In the Standard Model (SM), the decays $B \to K^* \gamma$ [1] proceed dominantly through one-loop $b \to s\gamma$ electromagnetic penguin transitions. Some extensions of the SM predict new high-mass particles that can exist in the loop and alter the branching fractions from their SM predictions. Previous measurements of the branching fractions [2–4] are in agreement with and more precise than SM predictions [5–9], which suffer from large hadronic uncertainties.

The time-integrated CP ($\mathcal{A}$) and isospin (Δ_{0-}) asymmetries have smaller theoretical uncertainties [10], and therefore provide more stringent tests of the SM. They are defined by:

$$\mathcal{A} = \frac{\Gamma(\overline{B} \to \overline{K}^* \gamma) - \Gamma(B \to K^* \gamma)}{\Gamma(\overline{B} \to \overline{K}^* \gamma) + \Gamma(B \to K^* \gamma)}, \qquad (1)$$

$$\Delta_{0-} = \frac{\Gamma(\overline{B}^0 \to \overline{K}^{*0} \gamma) - \Gamma(B^- \to K^{*-} \gamma)}{\Gamma(\overline{B}^0 \to \overline{K}^{*0} \gamma) + \Gamma(B^- \to K^{*-} \gamma)}, \qquad (2)$$

where the symbol Γ denotes the partial width. The SM predictions for $\mathcal{A}$ are on the order of 1% [11], while those for Δ_{0-} range from 2 to 10% [8, 12]. However, new physics could alter these parameters significantly [12–14], and thus precise measurements can constrain those models. In this letter, we report measurements of $\mathcal{B}(B^0 \to K^{*0}\gamma)$, $\mathcal{B}(B^+ \to K^{*+}\gamma)$, Δ_{0-}, and $\mathcal{A}$. We use a data sample containing about 383 million $B\overline{B}$ events, corresponding to an integrated luminosity of 347 fb^{-1}, recorded at a center-of-mass (CM) energy corresponding to the $\Upsilon(4S)$ mass. The data was taken with the BABAR detector [15] at the PEP-II asymmetric e^+e^- collider. We also make use of events simulated using Monte Carlo (MC) methods and a GEANT4 [16] detector simulation. These results supercede the previous BABAR measurements [3].

$B \to K^* \gamma$ decays are reconstructed in the following K^* modes: $K^{*0} \to K^+\pi^-$, $K^{*0} \to K_S\pi^0$, $K^{*+} \to K^+\pi^0$, and $K^{*+} \to K_S\pi^+$. For each signal decay mode, the selection requirements described below have been optimized for the maximum statistical sensitivity of $S/\sqrt{S+B}$, where S and B are the rates for signal and background, respectively, where the assumed signal branching fraction is 4.0×10^{-5} [3]. The dominant source of background is continuum events ($e^+e^- \to q\bar{q}(\gamma)$, with $q = u, d, s, c$) that contain a high-energy photon from a π^0 or η decay or from an initial-state radiation (ISR) process. Backgrounds coming from $B\overline{B}$ events are mostly from higher-multiplicity $b \to s\gamma$ decays, where one or more particles have not been reconstructed, and from decays of one $B \to K^*\gamma$ mode that enter the signal selection of another mode by mis-reconstructing the K^* meson.

Photon candidates are identified as localized energy deposits in the calorimeter (EMC) that are not associated with any charged track. The signal photon candidate is required to have a CM energy between 1.5 and 3.5 GeV, to be well-isolated and to have a shower shape consistent with an individual photon [17]. In order to veto photons from π^0 and η decays, we form photon pairs composed of the signal photon candidate and all other photon candidates in the event. We then reject signal photon candidates consistent with coming from a π^0 or η decay based on a likelihood ratio that uses the energy of the partner photon, and the invariant mass of the pair.

Charged particles, except those used to form K_S candidates, are selected from well-reconstructed tracks that have at least 12 hits in the Drift Chamber (DCH), and are required to be consistent with coming from the $e^+ e^-$ interaction region. They are identified as K or π mesons by the Cherenkov angle measured in the Cherenkov photon detector (DIRC) as well as by energy loss of the track ($\mathrm{d}E/\mathrm{d}x$) in the silicon vertex tracker (SVT) and DCH. The K_S candidates are reconstructed from two oppositely charged tracks that come from a common vertex. In the $K^{*0} \to K_S\pi^0$ ($K^{*+} \to K_S\pi^+$) mode, we require the invariant mass of the pair to be $0.49 < m_{\pi^+\pi^-} < 0.52 \ \mathrm{GeV}/c^2$ ($0.48 < m_{\pi^+\pi^-} < 0.52 \ \mathrm{GeV}/c^2$) and the reconstructed decay length of the K_S to be at least 9.3(10) times its uncertainty.

We form π^0 candidates by combining two photons (excluding the signal photon candidate) in the event, each of which has an energy greater than 30 MeV in the laboratory frame. We require the invariant mass of the pair to be $0.112 < m_{\gamma\gamma} < 0.15 \ \mathrm{GeV}/c^2$ and $0.114 < m_{\gamma\gamma} < 0.15 \ \mathrm{GeV}/c^2$ for the $K^{*0} \to K_S\pi^0$ and $K^{*+} \to K^+\pi^0$ modes respectively. In order to refine the π^0 three-momentum vector, we perform a mass-constrained fit of the two photons.

We combine the reconstructed K and π mesons to form K^* candidates. We require the invariant mass of the pair to satisfy $0.78 < m_{K^+\pi^-} < 1.1 \ \mathrm{GeV}/c^2$, $0.82 < m_{K_S\pi^0} < 1.0 \ \mathrm{GeV}/c^2$, $0.79 < m_{K^+\pi^0} < 1.0 \ \mathrm{GeV}/c^2$, and $0.79 < m_{K_S\pi^+} < 1.0 \ \mathrm{GeV}/c^2$. The charged track pairs of the $K^{*0} \to K^+\pi^-$ mode are required to originate from a common vertex.

The K^* and high-energy photon candidates are combined to form B candidates. We define in the CM frame (the asterisk denotes a CM quantity) $\Delta E \equiv E_B^* - E_{\mathrm{beam}}^*$, where E_B^* is the energy of the B meson candidate and E_{beam}^* is the beam energy. The beam-energy-substituted mass is defined as $m_{\mathrm{ES}} \equiv \sqrt{E_{\mathrm{beam}}^{*2} - \mathrm{p}_B^{*2}}$, where p_B^* is the momentum of the B candidate. In addition, we consider the helicity angle θ_H of the K^*, defined as the angle between the momenta one of the daughters of the K^* meson and the B candidate in the K^* rest frame. The distribution of $\cos\theta_H$ is $\sin^2\theta$ for signal events. Signal events have ΔE close to zero with a gaussian resolution of approximately 50 MeV, and an m_{ES} distribution centered at the mass of the B meson with a gaussian resolution of approximately 3 MeV/c^2. We only consider candidates in
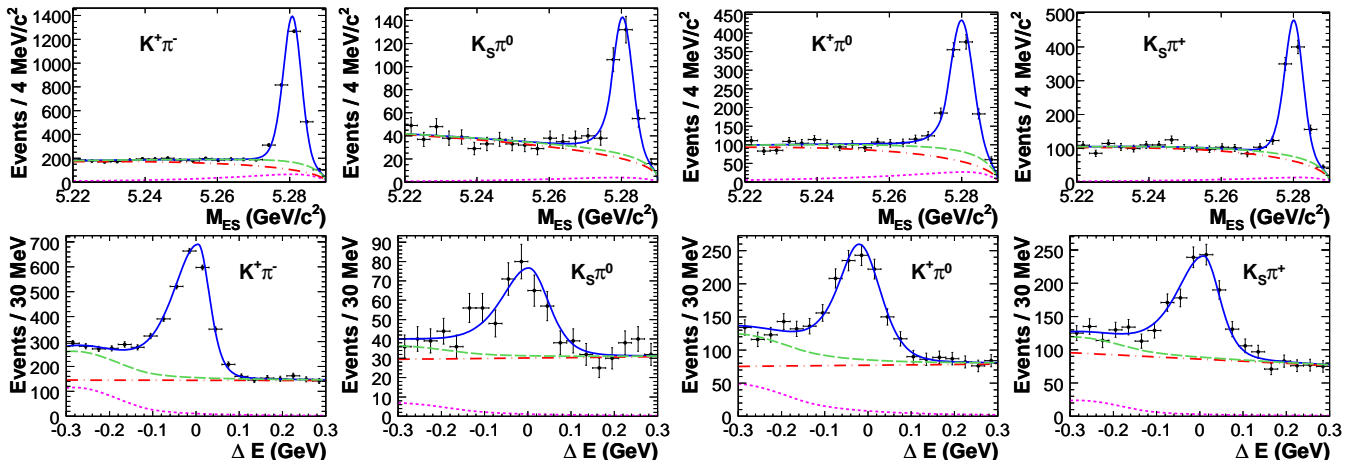
FIG. 1: m_{ES} and ΔE projections of the fits. The points are data, the solid line is the fit result, the dotted line is the $B\overline{B}$ background, and the dash-dotted line is the continuum background. The dashed line gives the total ($B\overline{B}$ and continuum) contribution to the background.

the ranges $-0.3 < \Delta E < 0.3$ GeV, $m_{\mathrm{ES}} > 5.22$ GeV/c^2, and $|\cos\theta_H| < 0.75$. To eliminate badly reconstructed events, we apply a loose selection criterion to the vertex separation (and its uncertainty) along the beam axis between the B meson candidate and the rest of the event (ROE). The ROE is defined as all charged tracks and neutral energy deposits in the calorimeter that are not used to reconstruct the B candidate.

In order to reject continuum background, we combine 13 variables into a neural network (NN). One class of these variables exploits the topological differences between isotropically distributed signal events and jet-like continuum events by considering correlations between the B meson candidate and the ROE. The other class exploits the fact that B meson decays tend to not conserve flavor, while continuum events tend to be flavor-conserving. The discriminating variables are described in Ref. [18]. Each signal mode has a separately trained neural network, whose output peaks at a value of one for signal-like events and zero for background-like events. A selection is made upon the output.

After applying all the selection criteria, there are, on average, ~ 1.1 B^0/B^+ candidates per event in simulated signal events. In events with multiple candidates, we select the candidate with the reconstructed K^* mass closest to the nominal K^* mass [21].

We perform an unbinned extended maximum likelihood fit to extract the signal yield, constructing a separate fit for each mode. Since the correlations among the three observables $(m_{\mathrm{ES}}, \Delta E, \cos\theta_H)_j$ are small, we use uncorrelated probability distribution functions (PDFs) each representing the observables to construct the likelihood function. The likelihood function is:

$$\mathcal{L} = \exp\left(-\sum_{i=1}^{M} n_i\right) \cdot \left(\prod_{j=1}^{N}\left[\sum_{i=1}^{M} n_i \mathcal{P}_i(\vec{x}_j;\ \vec{\alpha}_i)\right]\right)$$

where N is the number of events, $M = 3$ is the number of hypotheses (signal, continuum, and $B\overline{B}$), and n_i is the yield of a particular hypothesis. $\mathcal{P}_i$ is the product of one-dimensional PDFS over the three dimensions $\vec{x}$, and $\vec{\alpha}$ represents the fit parameters. All types of $B\overline{B}$ background are included in the $B\overline{B}$ component, which is suppressed by the use of $\cos\theta_H$. The signal m_{ES} distribution for the $K^{*0} \to K_S\pi^0$ and $K^{*+} \to K^+\pi^0$ modes is described by a Crystal Ball function [19], which has two tail parameters that are fixed to values obtained from MC. For the $K^{*0} \to K^+\pi^-$ and $K^{*+} \to K_S\pi^+$ modes, the signal m_{ES} distribution is parameterized as a piece-wise function $f(x) = \exp\left(-(x-\mu)^2/(\sigma_{L,R}^2 + \alpha_{L,R}(x-\mu)^2)\right)$, defined to the left (L) and right (R) of μ, which is the peak position of the distribution. Here, $\sigma_{L,R}$ and $\alpha_{L,R}$ are the widths and measures of the tails, respectively, to the left and right of the peak. We constrain $\sigma_L = \sigma_R$, which is floated, and fix $\alpha_{L,R}$ to values obtained from MC. This same function also describes the signal ΔE distribution for each mode, but with different values for the parameters. In addition, we allow σ_L and σ_R to float independently. The $\cos\theta_H$ distribution for the signal component is modeled by a 2$^{\mathrm{nd}}$ order polynomial, with all of its parameters floating in the fit. For the continuum hypothesis, the m_{ES} PDF is parameterized by an ARGUS function [20], with its shape parameter floating in the fit. The continuum ΔE and $\cos\theta_H$ shapes are modeled by a first- or second-order polynomial with its parameters floating in the fit. Various functional forms are used to describe the $B\overline{B}$ background, all parameters of which are taken from MC simulation and held fixed. All of the

TABLE I: The signal reconstruction efficiency ϵ, the fitted signal yield N_S, branching fraction, $\mathcal{B}$, and CP asymmetry, $\mathcal{A}$, for each decay mode. Errors are statistical and systematic, with the exception of ϵ and N_S, which have only systematic and statistical errors, respectively.

Mode	$\epsilon(\%)$	N_S	$\mathcal{B}(\times 10^{-5})$	Combined $\mathcal{B}(\times 10^{-5})$	$\mathcal{A}$	Combined $\mathcal{A}$
$K^+\pi^-$	21.8 ± 0.8	2400.0 ± 55.4	$4.45\pm0.10\pm0.17$	$\Big\}\,4.47\pm0.10\pm0.16$	$-0.016\pm0.022\pm0.007$	
$K_s\pi^0$	13.0 ± 0.9	256.0 ± 20.6	$4.66\pm0.37\pm0.35$			$\Big\}-0.003\pm0.017\pm0.007$
$K^+\pi^0$	15.3 ± 0.8	872.7 ± 37.6	$4.38\pm0.19\pm0.26$	$\Big\}\,4.22\pm0.14\pm0.16$	$+0.040\pm0.039\pm0.007$	
$K_s\pi^+$	20.1 ± 0.7	759.1 ± 33.8	$4.13\pm0.18\pm0.16$		$-0.006\pm0.041\pm0.007$	

component yields are floating.

Figure 1 and Table I show the results of the likelihood fit to data. The branching fractions have been obtained using $\mathcal{B}(\Upsilon(4S) \to B^0\overline{B}^0) = 0.484 \pm 0.006$, $\mathcal{B}(\Upsilon(4S) \to B^+B^-) = 0.516 \pm 0.006$ [21]. Also shown are the combined branching fractions, which have been calculated taking into account correlated systematic errors.

The CP asymmetry $\mathcal{A}$ is measured in three modes: $K^{*0} \to K^+\pi^-$, $K^{*+} \to K^+\pi^0$, and $K^{*+} \to K_S\pi^+$. In each of these modes, the final state of the signal B meson is determined by its final state daughters. The fit is accomplished by performing a simultaneous fit to the two flavor sub-samples (K^* and $\overline{K}^*$) in each mode. All shape parameters are assumed to be flavor independent and the $\mathcal{A}$ of each component is floated in the fit. Table I gives the individual and combined $\mathcal{A}$ results.

Table II lists the sources of systematic uncertainty for the branching fractions for all four modes. The "Fit Model" systematic incorporates uncertainties due to imperfect knowledge of the normalization and shape of the inclusive $B \to X_s\gamma$ spectra, and the choice of fixed parameters. The "Signal PDF bias" systematic uncertainty characterizes any bias resulting from correlations among the three observables, or incorrect modeling of the signal PDFs. The remaining sources of error on the signal efficiency are studied using control samples in the data. From all of these studies, we derive signal efficiency correction factors and associated uncertainties. The total corrections are 0.953, 0.897, 0.919, and 0.936 for the $K^{*0} \to K^+\pi^-$, $K^{*0} \to K_S\pi^0$, $K^{*+} \to K^+\pi^0$, and $K^{*+} \to K_S\pi^+$ modes, respectively. The systematic error on $\mathcal{A}$ comes largely from the uncertainty in the charge asymmetry of the hadronic interaction of the final state mesons with the detector material.

We combine the branching fractions and the ratio of the B^+ and B^0 lifetime $\tau_+/\tau_0 = 1.071 \pm 0.009$ [21] to obtain the isospin asymmetry $\Delta_{0-} = 0.066 \pm 0.021 \pm 0.022$, which corresponds to $0.017 < \Delta_{0-} < 0.116$ at the 90% confidence interval. We also measure $\mathcal{A}(B^+ \to K^{*+}\gamma) = 0.018 \pm 0.028 \pm 0.007$. The total combined CP asymmetry is $\mathcal{A} = -0.003 \pm 0.017 \pm 0.007$, with a 90% confidence interval of $-0.033 < \mathcal{A} < 0.028$.

Figure 2 shows the relativistic P-wave Breit-Wigner line shape fit to the sPlot [22] of the $K\pi$ invariant mass

distribution of data projecting out the signal component. For the $K^{*0} \to K_S\pi^0$ and $K^{*+} \to K^+\pi^0$ modes, we convolve the Breit-Wigner line shape with a Gaussian with a width of 10 MeV (determined from MC simulation) to account for detector resolution. For the $K^{*0} \to K^+\pi^-$ and the $K^{*+} \to K_S\pi^+$ modes, the detector resolution is negligible. The results are consistent with the signal events containing only P-wave K^* mesons and no other $K\pi$ resonances.
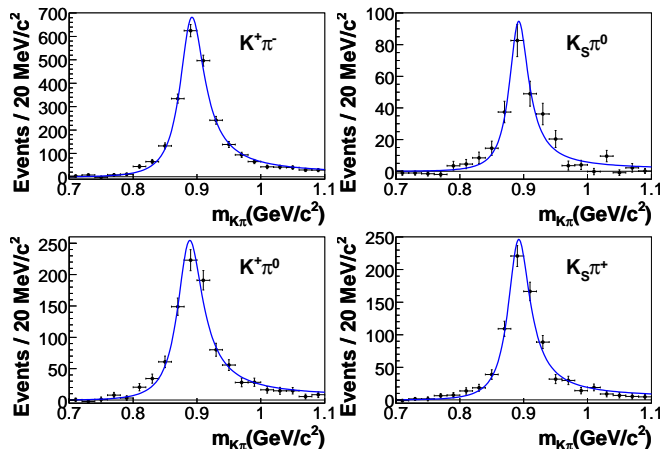

FIG. 2: Fit of a single relativistic P-wave Breit-Wigner line shape (solid line) to the $K\pi$ invariant mass distribution of the sPlot of data (points). For the $K^{*0} \to K_S\pi^0$ and $K^{*+} \to K^+\pi^0$, the Breit-Wigner is convolved with a Gaussian of width 10 MeV.

We conclude that using a sample that is almost five times larger than previously used, we have signficantly improved upon previous measurements of the $B \to K^*\gamma$ decay processes [2–4]. The measured isospin- and CP-asymmetries and branching fractions are consistent with SM expectations.

TABLE II: Systematic errors (in %) of the branching fractions.

Mode	$K^+\pi^-$	$K_S\pi^0$	$K^+\pi^0$	$K_S\pi^+$
$\mathcal{B}(\Upsilon(4S)\to B^0\overline{B}^0)/\mathcal{B}(\Upsilon(4S)\to B^+B^-)$	1.6	1.6	1.6	1.6
$B\overline{B}$ sample size	1.1	1.1	1.1	1.1
Tracking efficiency	1.2	-	0.6	0.8
Particle identification	0.6	-	0.6	0.2
Photon selection	2.2	2.2	2.2	2.2
π^0 reconstruction	-	3.0	3.0	-
π^0 and η veto	1.0	1.0	1.0	1.0
K_S reconstruction	-	0.7	-	0.7
Neural Net efficiency	1.5	1.0	1.0	1.0
Fit Model	0.8	5.6	3.1	1.7
Signal PDF bias	0.9	2.2	1.6	1.4
Sum in quadrature	3.9	7.5	5.7	4.1

[*] Deceased

[†] Now at Temple University, Philadelphia, Pennsylvania 19122, USA

[‡] Also with Università di Perugia, Dipartimento di Fisica, Perugia, Italy

[§] Also with Università di Roma La Sapienza, I-00185 Roma, Italy

[¶] Now at University of South Alabama, Mobile, Alabama 36688, USA

[**] Also with Laboratoire de Physique Nucléaire et de Hautes Energies, IN2P3/CNRS, Université Pierre et Marie Curie-Paris6, Université Denis Diderot-Paris7, F-75252 Paris, France

[††] Also with Università di Sassari, Sassari, Italy

[1] K^* refers to the $K^*(892)$ resonance throughout this paper.
[2] T. E. Coan et al., Phys. Rev. Lett. **84**, 5283 (2000).
[3] B. Aubert et al. (BABAR Collaboration), Phys. Rev. D **70**, 112006 (2004).
[4] M. Nakao et al., Phys. Rev. D**69**, 112001 (2004).
[5] A. Ali and A. Y. Parkhomenko, Eur. Phys. Jour. C **23**, 89 (2002).
[6] S. W. Bosch and G. Buchalla, Nucl. Phys. B **621**, 459 (2002).
[7] M. Beneke, T. Feldmann, and D. Seidel, Nucl. Phys. B **612**, 25 (2001).
[8] M. Matsumori, A.I. Sanda, and Y.-Y. Keum, Phys. Rev. D **72**, 014013 (2005).
[9] A. Ali, B. Pacjak, and C. Greub, Eur. Phys. Jour. C **55**, 577 (2008).
[10] Charge conjugate modes are implied throughout, except for the CP asymmetry.
[11] C. Greub, H. Simma, and D. Wyler, Nucl. Phys. B **434**, 39 (1995).
[12] A. L. Kagan and M. Neubert, Phys. Lett. B **539**, 227 (2002).
[13] M. R. Ahmady and F. Mahmoudi, Phys. Rev. D **75**, 015007 (2007).
[14] C. Dariescu and M. Dariescu, arXiv:0710.3819 [hep-ph].
[15] B. Aubert et al. (BABAR Collaboration), Nucl. Instrum. Methods A **479**, 1 (2002).
[16] S. Agostinelli et al., Nucl. Instrum. Methods A **506**, 250 (2003).
[17] B. Aubert et al. (BABAR Collaboration), Phys. Rev. Lett. **88**, 101805 (2002).
[18] B. Aubert et al. (BABAR Collaboration), Phys. Rev. Lett. **98**, 151802 (2007).
[19] M. J. Oreglia, Ph.D Thesis, SLAC-236 (1980), J. E. Gaiser, Ph.D. Thesis, SLAC-255 (1982).
[20] H. Albrecht et al., Z. Phys. C **48**, 543 (1990).
[21] C. Amsler et al. (Particle Data Group), Physics Letters **B667**, 1 (2008).
[22] M. Pivk and F. R. Le Diberder, Nucl. Instrum. Meth. A **555**, 356 (2005).